



# Numerical simulation study on impact factors to dynamic filtration loss

Cuilong Kong<sup>1,2</sup> · Yuxue Sun<sup>1</sup> · Chengli Li<sup>3</sup> · Jingyuan Zhao<sup>1</sup> · Xiuyu Zhu<sup>4</sup>

Received: 13 April 2023 / Accepted: 30 October 2023 / Published online: 8 January 2024  
© The Author(s) 2024

## Abstract

During drilling operations, naturally, fractured formations are prone to show serious mud losses, which hinder drilling and increase nonproductive time and costs. The influencing factors of dynamic fluid loss are important for optimizing drilling parameters, reducing drilling fluid loss, and protecting oil and gas reservoirs. In this study, we simulated the dynamic filtration loss of drilling fluid during drilling under formation conditions using commercial software CMG (Computer Modelling Group). The effects of filtration time, filtrate viscosity, pressure difference, internal filter cake permeability, and external filter cake permeability on filtration loss were investigated. The simulation results showed that the permeability of the external mud cake is an important factor to control the fluid loss, and the pressure consumed by the external mud cake with low permeability can account for more than 90% of the total pressure difference. When the permeability of the external mud cake is high, the permeability of the internal mud cake also has a significant influence on the dynamic fluid loss. Under formation conditions, the dynamic fluid loss of radial fluid loss is still proportional to the filtration time and pressure difference, and inversely proportional to the filtrate viscosity of drilling fluid. Under the simulated conditions, the pressure will quickly transfer to the boundary, and the formation pressure at the same position in the formation will gradually increase, while the increase is relatively small with a constant filtration rate. The results of this paper can be used to the real site for drilling optimization. This numerical analysis method can be easily applied to filtrate loss analysis, formation damage area calculation, and other radial flow-related study.

**Keywords** Numerical simulation · Dynamic filtration loss · Drilling fluid

## List of symbols

$A$	Area of filter cake, $m^2$
$c_p$	Mass of particles per unit volume of carrier fluid in slurry, $g/cm^3$
$K$	Permeability, $m^2$
$K_{ec}$	External filter cake permeability, $mD (\times 10^{-3} \mu m^2)$
$K_{ic}$	Internal filter cake permeability, $mD (\times 10^{-3} \mu m^2)$
$k_d$	Deposition coefficient, dimensionless

$k_e$	Erosion coefficient, $s/cm$
$L$	Thickness of filter cake, $m$
$q$	Flow rate of filter fluid, $m^3/s$
$r_c$	Filter cake radius, $cm$
$t$	Filtration time, $s$
$u_c$	Fluid flux at the cake surface, $cm/s$
$P_f$	Original formation pressure, $MPa$
$P_h$	Drilling fluid column pressure, $MPa$
$\Delta p$	Pressure difference, $MPa$

✉ Chengli Li  
1139406976@qq.com

<sup>1</sup> Key Laboratory of the Ministry of Education for Improving Oil and Gas Recovery, Northeast Petroleum University, Daqing 163318, China

<sup>2</sup> Oil Production Engineering Research Institute of Daqing Oilfield, Daqing 163453, China

<sup>3</sup> Tarim Oilfield Company, Xinjiang 841599, China

<sup>4</sup> Drilling Engineering Technology Research Institute of Daqing Oilfield Drilling Engineering Company, Daqing 163355, China

## Greek symbols

$\beta$	Inertial flow coefficient for the rock or filter cake, dimensionless
$\mu$	Viscosity of fluid, $mPa \cdot s$
$\mu_o$	Crude oil viscosity, $mPa \cdot s$
$\mu_f$	Drilling fluid filtrate viscosity, $mPa \cdot s$
$\tau_{cr}$	Critical shear stress, $dynes/cm^2$
$\tau_s$	Slurry shear stress at the cake surface, $dynes/cm^2$
$\rho_p$	Particle mass density, $g/cm^3$
$\phi_c$	Filter cake porosity, %

## Introduction

The drilling fluid is the first foreign fluid contacting the formation. During the drilling process, the column pressure of the drilling fluid is often higher than the formation pressure to ensure drilling safety. When the reservoir is drilled open, the solid phase particles in the mud, treatment agent, and filtrate enter the formation due to pressure differences, leading to a change in formation fluid saturation. A physicochemical reaction occurs between the filtrate, minerals, and matrix in the pore space, leading to damaged oil and gas formation and decreased permeability close near-bore zones, which increases the flow resistance for the crude oil flowing to the wellbore and impacts the capacity of oil and gas wells (Kuang et al. 2010; Fan et al. 2018). As a result, problems may emanate because of the severity of lost fluid, wellbore instability, formation damage, and sometimes freshwater aquifer contamination (Al-Hameedi et al. 2019; Seyedmohammadi 2017). Significant mud loss may hamper operations and increase nonproductive time and cost (Amadi-Echendu and Yakubu 2012).

During the entire drilling process, the largest proportion of filtration loss and longest duration happens during dynamic filtration, accounting for approximately 80–90% of the total filtration loss (Yan 2011). By studying the influencing factors relevant to the dynamic filtration loss, we can guide the optimal formulation of the drilling fluid, optimize the relevant parameters, and reduce the filtration loss of the drilling fluid to protect the oil and gas reservoir. Martins et al. (2007) discussed the optimization of viscoelastic parameters and performed an intrusion analysis based on two-phase (viscoelastic fluid + Newton oil) radial flow through porous media and commercial CFD software. A different concept was proposed to control the intrusion, designing a polymer-based fluid that generates extremely high frictional losses when flowing through a porous medium, but no additional losses in the wellbore. To achieve fluid flow and solid transport properties in the well without intruding into the rock formation, Wang et al. (2020a, b) developed an efficient drilling fluid for coal seam methane drainage boreholes. Okoro et al. (2020) used ANN (artificial neural network) to predict the rheological properties. Different concentrations of the nanoparticles were added to these suspensions of water to act as filtration loss materials. A reservoir non-damaging nano-treated aqueous-based drilling fluid was proposed. Majidi et al. (2010) gave a theoretical solution for the radial flow of a yield-power-law fluid between two parallel disks based on the momentum balance in the radial coordinate system. By mathematical simplification, the closed expression of radial flow pressure drop of power-law fluid is obtained, and the approximate analytical solution is given. The application of the approximate

solution in the prediction of fluid loss in fractured formation is discussed. Ahmad et al. (2018) studied the rheological and filtration properties of Bent/polymer dispersions in deionized and salt water at different temperatures (25 °C and 85 °C). The steady shear rheological data were fitted to Herschel–Bulkley model to compute rheological parameters like yield stress, consistency index, and flow behavior index. Kemerli and Engin (2021) evaluated the analytical and numerical modeling of the flow of Herschel–Bulkley fluid model in a monotube. Based on the fundamental principles of fluid mechanics, Wang et al. (2020b) established the control equation of liquid–solid multiphase flow in a 2D rough-walled stationary fracture. The drilling fluid was treated as a Bingham type non-Newtonian fluid, and the influence of solid particles on fluid flow was analyzed in detail. The finite difference method was adopted to the numerical solution of the equations, and the impact of such working parameters as fracture dimensions, bottom hole pressure differential, physical properties of both fluid and particle on the fluid loss were analyzed. Albattat and Hoteit (2019) based on the Cauchy momentum equation and considered key primary flow mechanisms, including the non-Newtonian behavior of drilling fluids using a power-law model, to establish a fluid dynamics model from the wellbore to the surrounding fractured medium. Dokhani et al. (2020) presented a mathematical model for predicting mud loss in naturally fractured formations. The mathematical model helps to qualitatively predict the amount of mud loss during well planning and quantify the diversion fractures in order to design effective fluid loss control materials. Albattat and Hoteit (2019, 2021) proposed a new semi-analytical solution for the fluid loss of non-Newtonian drilling fluids in fractured formations and demonstrated the applicability of the model. To solve the underground uncertainty, the semi-analytic solution is combined with the Monte Carlo method, and probabilistic prediction is generated. Andr' et al. (Soares et al. 2021) used the Herschel–Bulkley model to adjust rheological data. Rheological properties were improved by adding materials to combat loss of circulation (LCM) into the drilling fluid. The results showed that carboxymethylcellulose polymer (CMC), bentonite (BT), and hydrogel (HG) played a major role in plugging the fluid in the fracturing and filtration stages. Based on rheological tests, the interaction between HG\*CMC and BT\*CMC is important in preventing loss. When evaluating fluid loss in drilling fluid flow, most conclusions are that one-way fluid loss carried out under laboratory conditions to make an indoor evaluation (Bahrami et al. 2011; Byrne et al. 2010), while in the actual drilling process, dynamic fluid loss is a radial fluid loss process, and there is a certain deviation between the evaluation made under laboratory conditions and field situations (Lu et al. 2006; Won et al. 2008; Shan et al. 2014; Ding et al. 2007).

In this study, we use commercial software CMG to establish unidirectional filtration loss model and extend the model by considering the compressibility of rocks and fluids to simulate the process of radial dynamic filtration loss by drilling fluids under formation conditions. The simulation results are validated by experimental results. Then, the influencing factors of dynamic filtration loss were investigated using the model. The purpose of this paper is to provide insights into the main impact factors on drilling fluid filtration radial loss. Based on our research, the rank of impacting factors can be obtained, also for some impact factors, at a certain degree the filtration would show a sharp turn in trends, this can give the stimulation limits for field, could be a guidance for the field drilling design.

## Methodology

The main objective of this study was to investigate the influential factors of radial filtration loss of the drilling fluid under formation conditions. A unidirectional filtration loss numerical model was developed, and in order to verify model its accuracy, the results are compared with indoor experiments. The indoor experiments mainly used high-temperature and high-pressure dynamic filtration loss instruments and five artificial cores.

## Experimental study

### Materials and methods

The high-temperature and high-pressure multi-functional dynamic filtration meter can simulate the filtration loss of the drilling fluid under different temperatures and pressures. The instrument consists of the following parts: experimental main body system, pressure regulator system, stirring system, control system, support system, and cooling system. The main body of the experiment system is a high-temperature and high-pressure body with a volume of 800 ml and a heating device and a cooling device. The booster pressure regulator system includes nitrogen cylinders, low pressure pumps, high-pressure pumps, oil storage tanks, pressure converters, and pressure

lines. There are three kinds of pressurization methods in this instrument, nitrogen cylinder pressurization is adopted in this paper. The control system is mainly an industrial computer touch screen computer and various sensors (pressure sensor, temperature sensor, and photoelectric speed sensor). Various sensors can feed back parameters such as kettle temperature, kettle pressure, and agitator speed to the computer, and can read the data on the computer LCD screen. The experiment subjects were five artificial cores, denoted by numbers 1–5. The parameters of artificial cores are shown in Table 1. Before the experiment, the drilling fluid was stirred on a high-speed mixer for one minute. In the experiment, the filtration loss temperature was set to 50 °C, while the differential pressure was set to 2 MPa. The core was placed in the core holder and filtered for a while. After the filtration loss rate is stable (to ensure that it had reached the state of dynamic filtration loss), the filtration loss within a certain period of time was measured. Five artificial cores were tested in the laboratory for filtration loss, Figs. 1, 2 and 3 are multi-functional dynamic filtration device, artificial cores and pictures of filter cakes from experiments.

## Experimental results

In this study, the dynamic filtration test of five artificial cores under stratum conditions is studied. The results are shown in Table 1, which are the high-temperature and high-pressure dynamic filtration experiments of five artificial cores with different parameters under the same conditions. It can be seen that the amount of filtration increases generally with the increase in core permeability. However, the mud cake permeability is much lower than the formation permeability, so the influence of formation permeability on the fluid loss is not considered in this study. The reason for this phenomenon is that before the formation of mud cake, the formation is the first permeable medium for mud filtration.

The permeability of filter cake is calculated based on Darcy law, as shown in Eq. (1), all the parameters needed can be obtained from dynamic filtration loss experiments.

$$K = \frac{q\mu L}{\Delta p A} \quad (1)$$

**Table 1** Experimental results and related parameters

No	Diameter/cm	Length/cm	Core permeability/mD	Thickness of external filter cake/mm	Permeability of external filter cake/ $\times 10^{-3}$ mD	Filtration time/min	Filtration/mL
1	2.51	5.44	233	1.75	3.75	60	51
2	2.47	5.52	175	1.63	4.21	60	59
3	2.54	5.48	108	1.32	5.60	60	103
4	2.56	5.60	351	1.82	7.22	60	98
5	2.44	5.47	152	1.38	3.58	60	58



**Fig. 1** High-temperature and high-pressure multi-functional dynamic filtration for drilling fluid



**Fig. 2** Artificial cores

$K$  is permeability ( $\text{m}^2$ ),  $q$  is the flow rate of filter fluid ( $\text{m}^3/\text{s}$ ),  $\mu$  is viscosity of filter fluid ( $\text{mPa s}$ ),  $L$  is the thickness of filter cake (m) when the thickness is stable,  $\Delta p$  is the pressure difference (MPa), and  $A$  is the area of filter cake ( $\text{m}^2$ ).

Table 1 shows that the filtration loss of drilling fluid was reduced by reducing the permeability of the external filter cake, when other parameters are similar. Based on Darcy

law, when the thickness of filter cake is higher, extra percolating resistance caused by thicker filter cake exists, while under the same differential pressure and time duration, a slightly reduced filter loss is measured for No.4, but still close to the filter loss for No.3. Based on Eq. (1), when differential pressure  $\Delta p$  stays the same, smaller flow rate  $q$  but larger filter cake thickness  $L$ , will lead to a higher permeability. So, a higher permeability of No.4 is obtained. This demonstrates that the higher permeability could bring about higher filtration rate, which in turn also results in deposition of thicker filter cake, for which it could eventually lower the fluid loss.

### One-way filter loss model and validation

The established unidirectional filtration loss model is shown in Fig. 4, with the external filter cake as the first grid on the leftmost side and the core is divided into 20 grids. Considering the extremely low permeability of the external filter cake measured in the experiment, the influence of the internal filter cake on the filtration loss process is minimal. Thus, the influence of the internal filter cake is neglected in the unidirectional filtration loss model. In the unidirectional filtration loss model, all input parameters were kept consistent with the experimental conditions. The simulation and experimental results for the five cores are compared in Table 2.

The relative error of the four groups is within 5.0%, while that for one group is within 5.5%. The relative error between the simulation and experimental results is not significant, indicating the accuracy of the linear model.

Based on the verified linear model, a radial model under stratigraphic conditions is developed using the same method to investigate the influencing factors during dynamic filtration loss under stratigraphic conditions.

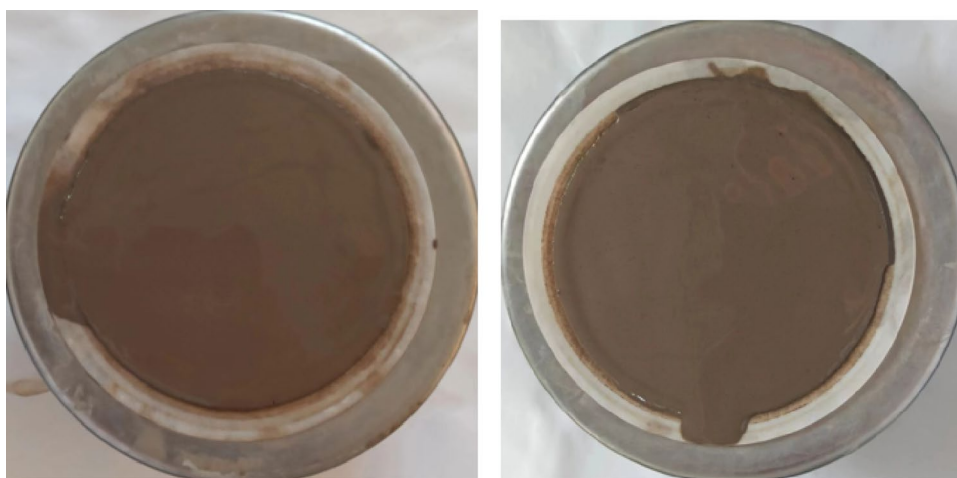
### Numerical study of radial dynamic filtration

The drilling fluid filtrate mainly invades the near-well zone. A radial grid, encrypted in the near-well area, is used to obtain the detailed distribution of pressure and water saturation in the near-well zone. The encrypted grid is divided as shown in Fig. 5 (the black area represents the encrypted grid line). The following assumptions were made: Dynamic condition is created by only drill pipe/shaft rotation (one-dimensional radial flow). Incompressible carrier fluid, particles, and uniform filter cake evolution. Negligible rock heterogeneity and mineralogical effect. The basic mathematical model includes material balance, Eq. (2).

$$-dr_c = \frac{k_d u_c c_p - k_e (\tau_s - \tau_{cr})}{(1 - \phi_c) \rho_p} dt \quad (2)$$



Fig. 3 Pictures of filter cake



(a) Filter cake for Core No.1

(b) Filter cake for Core No.4

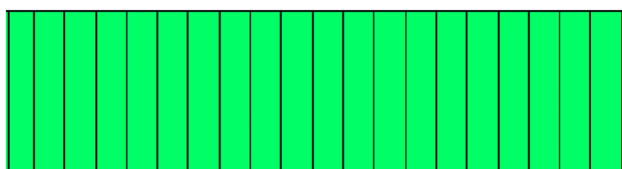


Fig. 4 Grid division of unidirectional filtration model

Table 2 Comparison between simulation results and experimental results

	Simulated filtration/mL	Experimental filtration/mL	Relative error/%
1	50	48	4.2
2	59	62	-4.8
3	103	105	-1.9
4	98	95	-3.1
5	58	55	5.5

where  $r_c$  is filter cake radius (cm),  $k_d$  is deposition coefficient (dimensionless),  $u_c$  is fluid flux at the cake surface (cm/s),  $c_p$  is mass of particles per unit volume of carrier fluid in slurry ( $\text{g}/\text{cm}^3$ ),  $k_e$  is erosion coefficient (s/cm),  $\tau_{cr}$  and  $\tau_s$  are critical shear stress and slurry shear stress at the cake surface ( $\text{dynes}/\text{cm}^2$ ), respectively,  $\rho_p$  is particle mass density ( $\text{g}/\text{cm}^3$ ),  $\phi_c$  is filter cake porosity (volume fraction), and  $t$  is filtration time.

Forchheimer equation is used as the motion equation, which accounts for the radial flow, and combining Forchheimer equation with the radial volumetric flux at the external filter cake surface gives Eqs. (2) and (3).

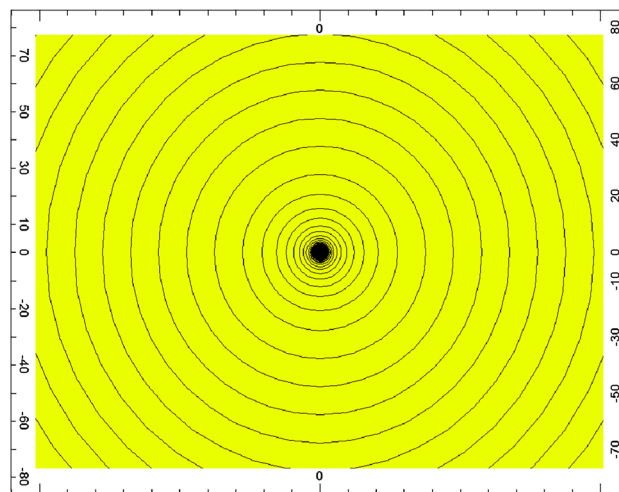


Fig. 5 Grid division diagram

$$-\frac{\partial p}{\partial r} = \frac{\mu}{2\pi h K} \frac{q}{r} + \frac{\beta \rho}{2\pi h^2} \left(\frac{q}{r}\right)^2 \tag{3}$$

$$\beta = \frac{2.92 \times 10^4}{\phi_{f/ec} K_{f/ec}} \tag{4}$$

where  $\mu$  is viscosity (mPa.s),  $K$  is permeability ( $\text{m}^2$ ),  $\beta$  is the inertial flow coefficient for the rock or filter cake (dimensionless),  $f$  represents formation, and  $ec$  represents external cake.

Simulation software is used to analyze the influence of different factors on dynamic filtration. The effects of the following five factors on dynamic filtration loss were analyzed, they are external filter cake permeability, differential pressure, drilling fluid filtrate viscosity, filtration

time, and internal filter cake permeability. We assumed that the formation permeability  $K$  is 100 mD, external filter cake thickness is 2 mm, internal filter cake thickness is 5 cm, internal filter cake permeability  $K_{ic}$  is 10 mD, original formation pressure  $P_f$  is 10 MPa, drilling fluid column pressure  $P_h$  is 12 MPa, formation crude oil viscosity  $\mu_o$  is 5 mPa·s, drilling fluid filtrate viscosity  $\mu_f$  is 1.5 mPa·s, borehole radius is 0.1 m (circular formation), boundary radius is 100 m, and the boundary condition is a closed boundary.

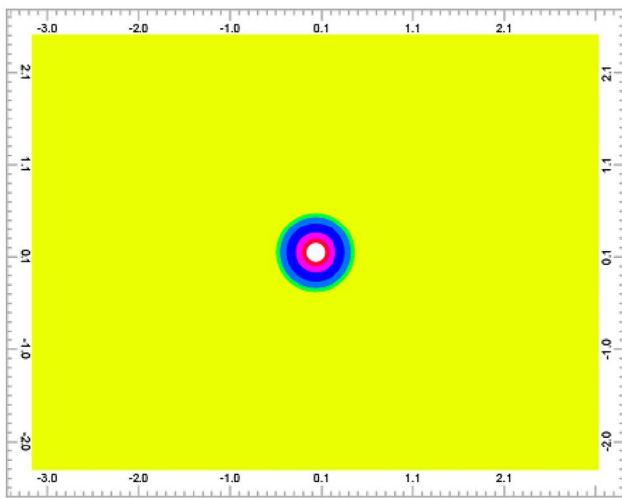
## Results and discussion

### Effect of the external filter cake permeability on the filtration loss

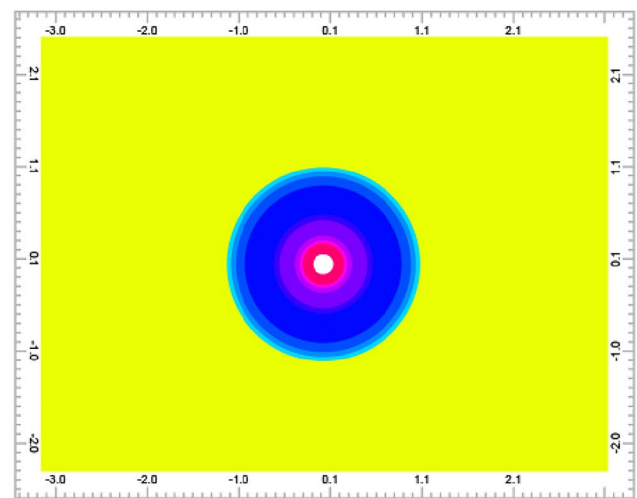
The effects of different external filter cake permeabilities  $K_{ec}$

**Table 3** Filtration and invasion depth under different permeability of external filter cake

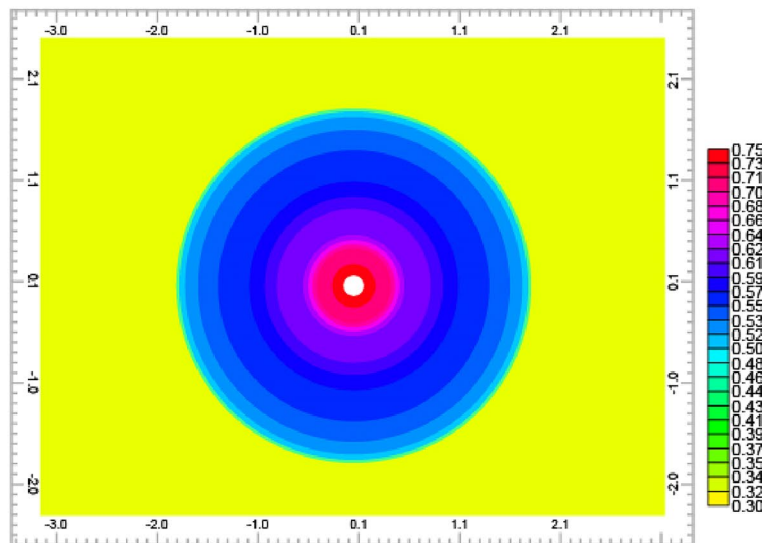
$K_{ec}$ /md	Filtration loss/m <sup>3</sup>
0.001	0.029662
0.01	0.278248
0.1	1.65999



(a)  $K_{ec}=0.001$  mD



(b)  $K_{ec}=0.01$  mD



(c)  $K_{ec}=0.1$  mD

**Fig. 6** Distribution of water saturation of near wellbore zone

on the invasion were investigated separately. The distribution of water saturation after 50 h is shown in Fig. 6, while the filtrate loss is shown in Table 3.

The filtration loss gradually increases with the external filter cake permeability. When the permeability of the external filter cake increased from 0.001 to 0.010 mD (a tenfold increase), the filtration loss also increased by a factor of approximately 10. When the permeability of the filter cake increased from 0.01 to 0.10 mD, the filtration loss increased by a factor of only approximately 6. This phenomenon can be explained by analyzing the pressure distribution in the near-well zone after 50 h (Fig. 7).

The pressure difference proportions consumed by the external filter cake for different external filter cake permeabilities are shown in Table 4. From the data here, we can see that the pressure difference proportion consumed by the

**Table 4** Differential pressure consumed by external filter cake

$K_{ec}$ /mD	Percentage of differential pressure consumed/%
0.001	99.2%
0.01	92.2%
0.1	55.1%

external filter cake decreases as the filter cake permeability increases under constant formation permeability. Therefore, the filtration loss does not exhibit a linear relationship with the filter cake permeability under constant total pressure difference. We can see from Fig. 8 that, when the permeability of external filter cake increases above 0.01 mD, the increase

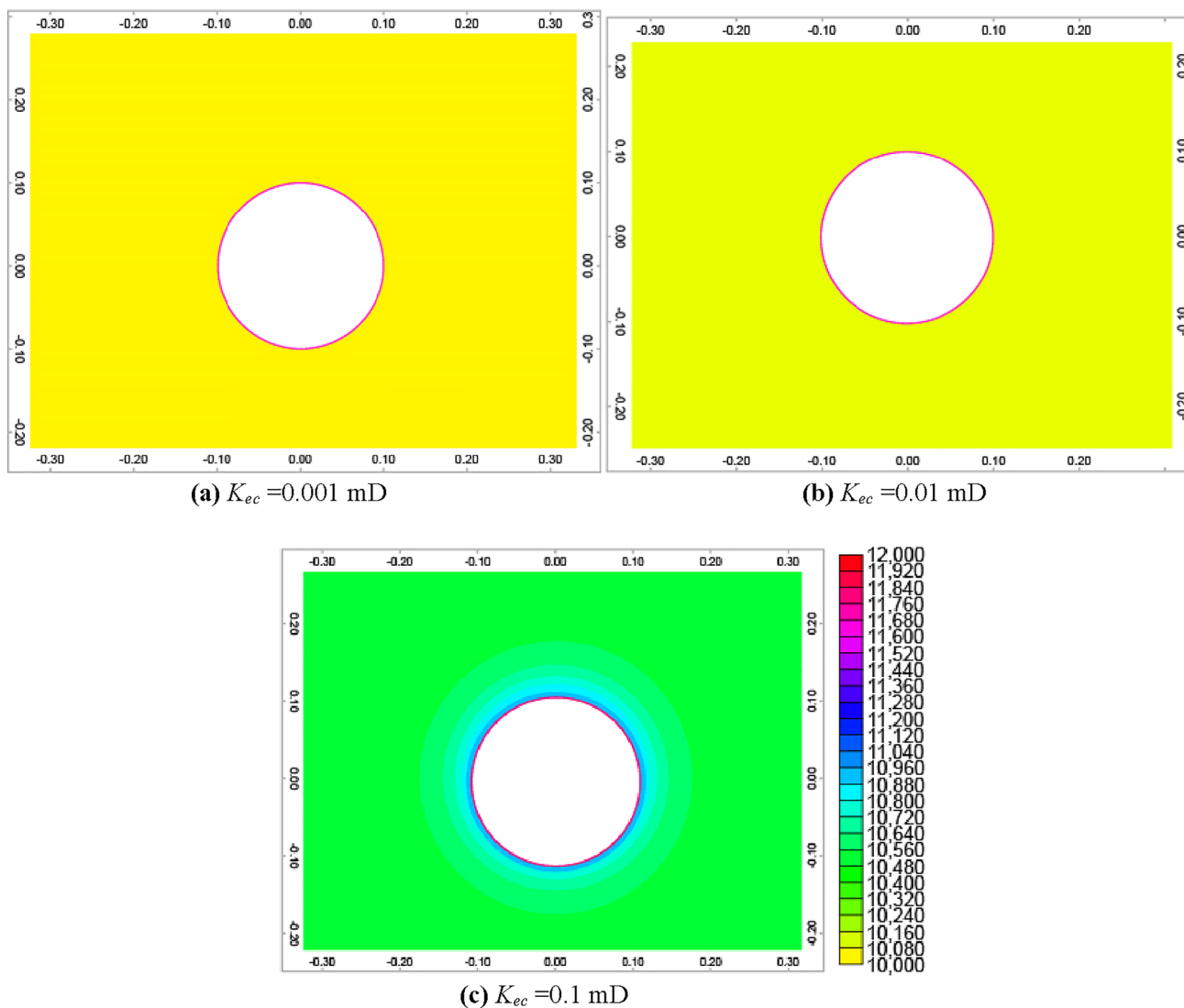


**Fig. 7** Pressure distribution of near wellbore zone

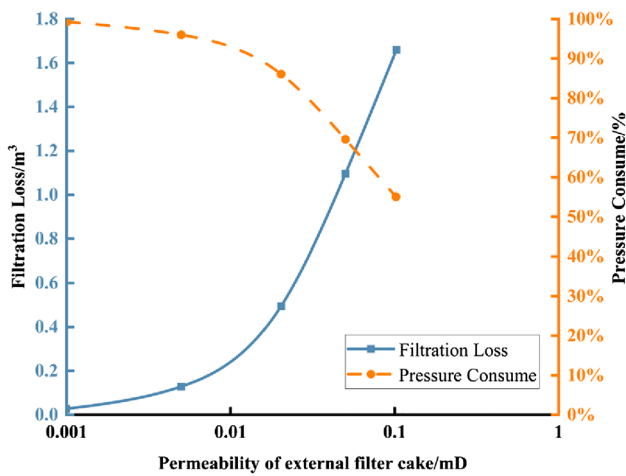


Fig. 8 Filtration loss and pressure consume along filter cake permeability changes

trend of filtration loss and the descent of pressure consuming over near bore are accelerated. This indicates the permeability limit of external filter cake, once the permeability exceeded the limit, a huge increment of filtration loss and pressure consuming occurs.

### Effect of the differential pressure on the filtration loss

According to the above simulation results, when the external filter cake permeability is 0.01 mD, the pressure consumed by the external filter cake accounts for more than 90% of the total differential pressure; in contrast, when the external filter cake permeability is smaller than 0.10 mD, the pressure consumed by the external filter cake is lower than 55% of the total differential pressure. The water saturation distribution after 50 h is shown in Fig. 9 and Fig. 10, while the corresponding filtration loss is shown in Fig. 11.

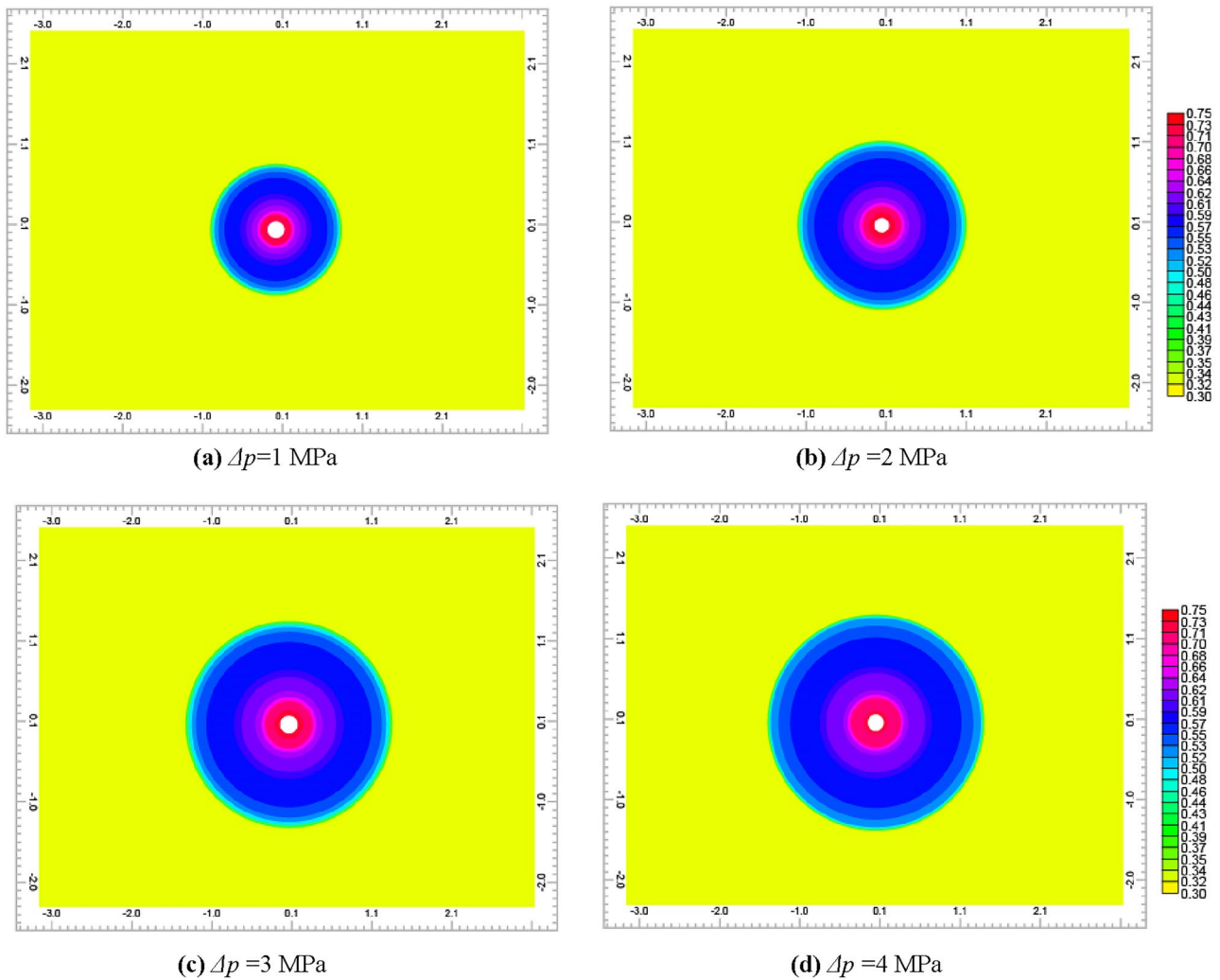


Fig. 9 Invasion under different differential pressures at the permeability of external filter cake of 0.01 mD



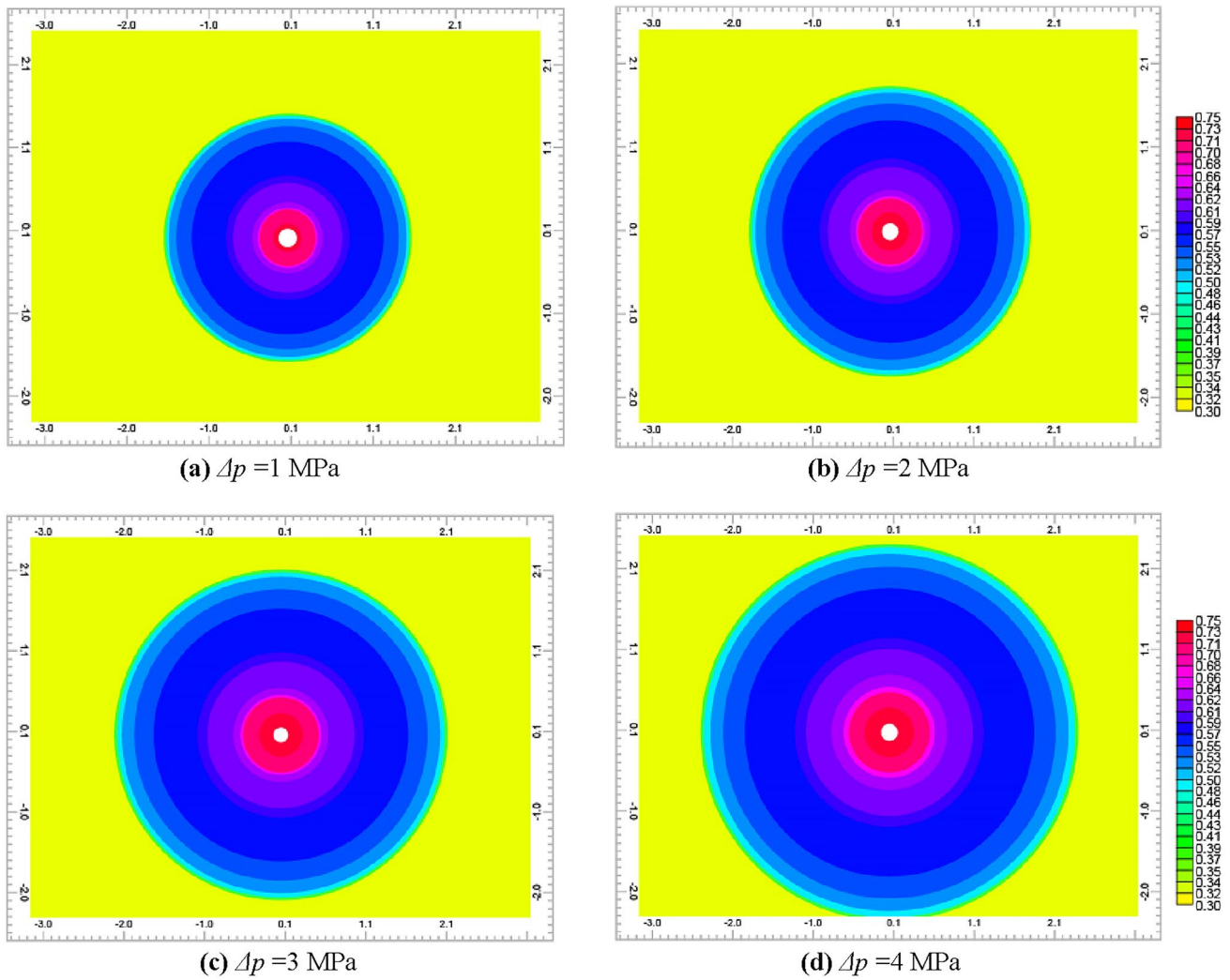


Fig. 10 Invasion under different differential pressures at the permeability of external filter cake of 0.1 mD

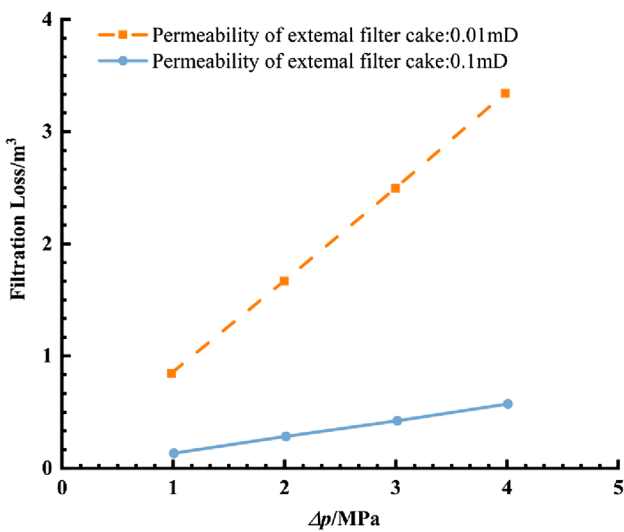


Fig. 11 Drilling fluid filtration under different permeability of external filter cake and different differential pressures

According to the simulation results, the filtration loss increases linearly with the pressure difference for external filter cake permeabilities of 0.01 and 0.10 mD. The increase in filtration loss is small for an external filter cake permeability of 0.01 mD because of the low filter cake permeability. The comparison of the distributions of formation pressure at different pressure differentials shows that the percentage change of the pressure differential consumed by the external filter cake to the total pressure differential was only 0.76% when the pressure differential changed from 1 to 4 MPa at an external filter cake permeability of 0.10 mD. The external filter cake consumed 0.49% pressure when the pressure differential changed from 1 to 4 MPa at an external filter cake permeability of 0.01 mD. With the change in the total differential pressure, the percentage of pressure consumed by the external filter cake to the total differential pressure is minimal. Thus, filtration loss increases linearly with the differential pressure for different external filter cake

permeabilities, this indicates that the flows through the filter cake follow Darcy law.

**Effects of the drilling fluid filtrate viscosity on the filtration loss and depth of invasion**

Assuming that  $\Delta p$  is 2 MPa,  $K_f$  is 100 mD,  $K_{ic}$  is 10 mD, and  $K_{ec}$  is 0.01 mD, the filtrate viscosity of the drilling fluid is varied to simulate the filtration loss of the drilling fluid under different filtrate viscosities. The distribution of water content saturation after 50 h is shown in Fig. 12. The filtration loss under different filtrate viscosities is shown in Fig. 13.

Figure 12 indicates that as the filtrate viscosity gradually increases, the filtration loss gradually decreases, and the rate of decrease gradually decreases. In addition, the filtration loss is approximately inversely proportional to the filtrate

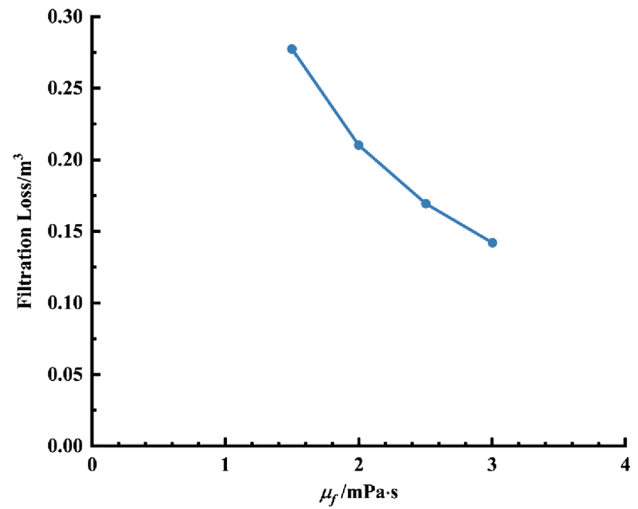


Fig. 13 Filtration under different filtrate viscosities

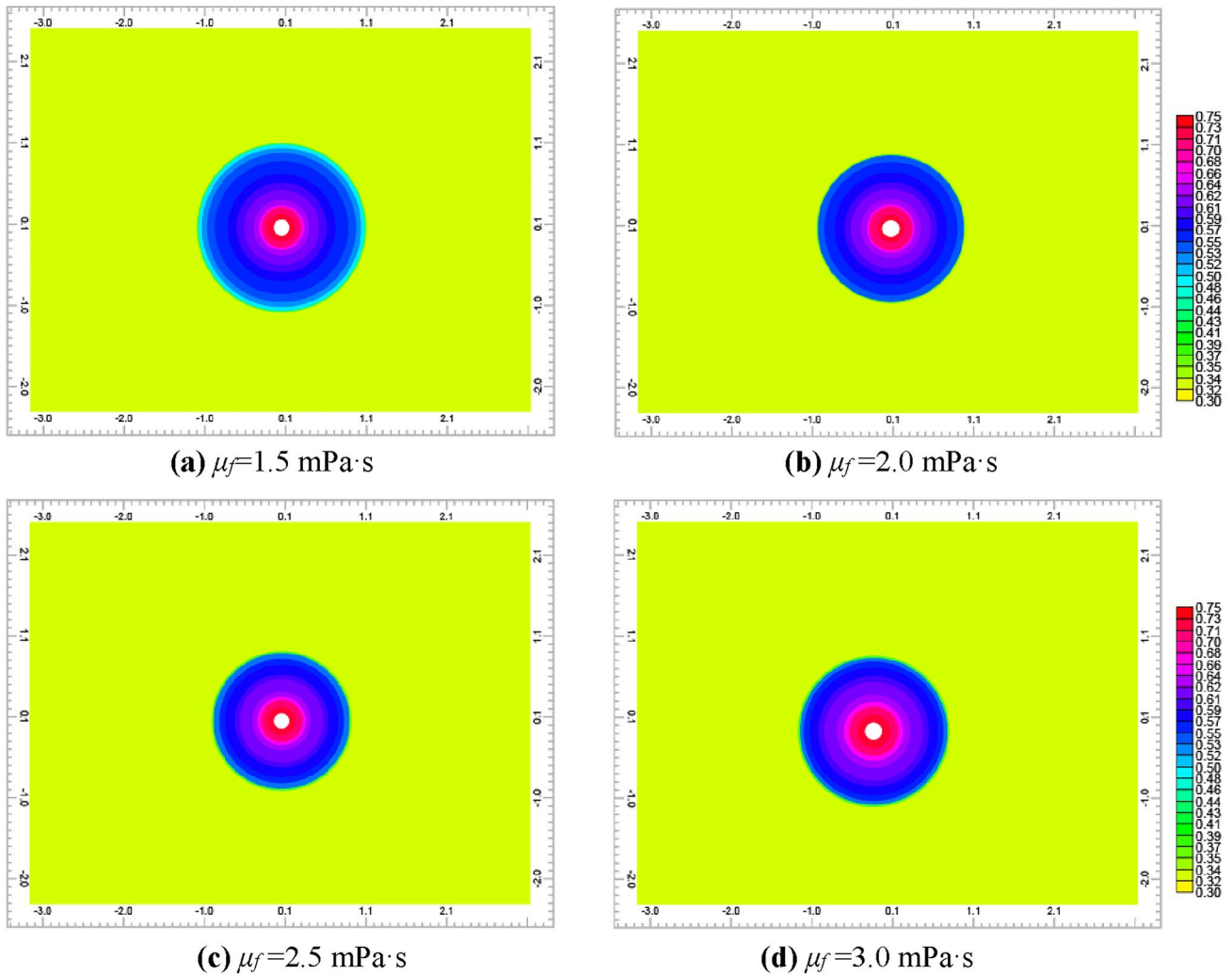


Fig. 12 Distribution of water saturation under different viscosities

viscosity. That is to say higher viscosity of the filtrate could lower the filtration loss.

### Effect of the filtration time on filtration loss

Under constant conditions as above, the filtration loss was simulated for various durations with external filter cake permeabilities of 0.01 mD and 0.10 mD by varying the permeability, with the simulation results shown in Fig. 14.

The filtration loss increases linearly with the time for both lower and higher permeabilities of the external filter cake, which also follows the Darcy law. At a permeability of the external filter cake of 0.01 mD, the increase in the filtration loss is small because of its low permeability. The distributions of differential pressure at different times are shown

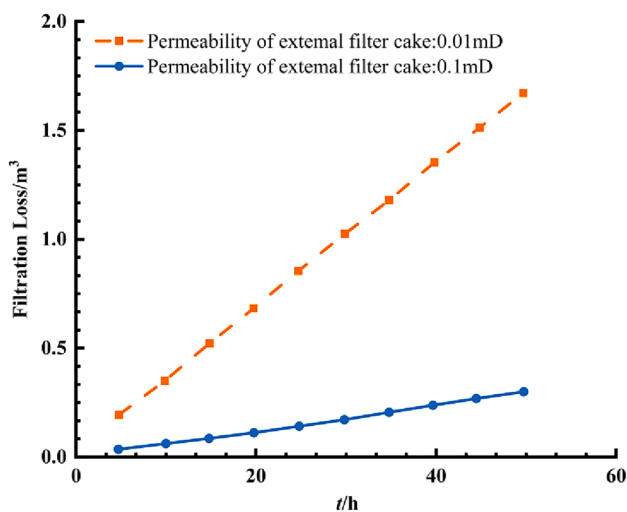


Fig. 14 Filtration under different filtrate durations

in Figs. 15 and 16. The comparison of the distributions of formation pressure at different times shows that the pressure is quickly transmitted to the boundary at filter cake permeabilities of 0.01 and 0.10 mD. With time, the drilling fluid filtrate continues to invade the formation, while the formation pressure at the same location in the formation gradually increases (however, the increase is relatively small). The pressure difference between the two ends of the filter cake at 5 and 50 h is 0.88% when the external filter cake permeability is 0.10 mD, and the pressure difference only 0.12% when the external filter cake permeability is 0.01 mD. Therefore, the filtration loss rate is essentially constant, while the filtration loss increases linearly with time.

### Effect of the internal filter cake permeability on the filtration loss

Before the external filter cake formation, the solid phase particles in the drilling fluid intrude into the reservoir and block the pore space of the formation around the borehole, resulting in a reduction in the permeability in the near-well zone. In severe cases, the permeability of the internal filter cake area can reduce 10% of the reservoir permeability. With the same conditions, only dynamic filtration loss changed from 10%, 30%, 50%, and 70% of the formation permeability for 50 h. The simulation results are shown in Fig. 17 and Fig. 18, and the corresponding filtration loss is shown in Table 3.

According to the simulation results and Table 5, with an increase in the internal filter cake permeability, the filtration loss also increases, but the rate of increase gradually decreases. The change in the internal filter cake permeability minimally affects the filtration loss when the external filter cake permeability is 0.01 mD. The change in the internal

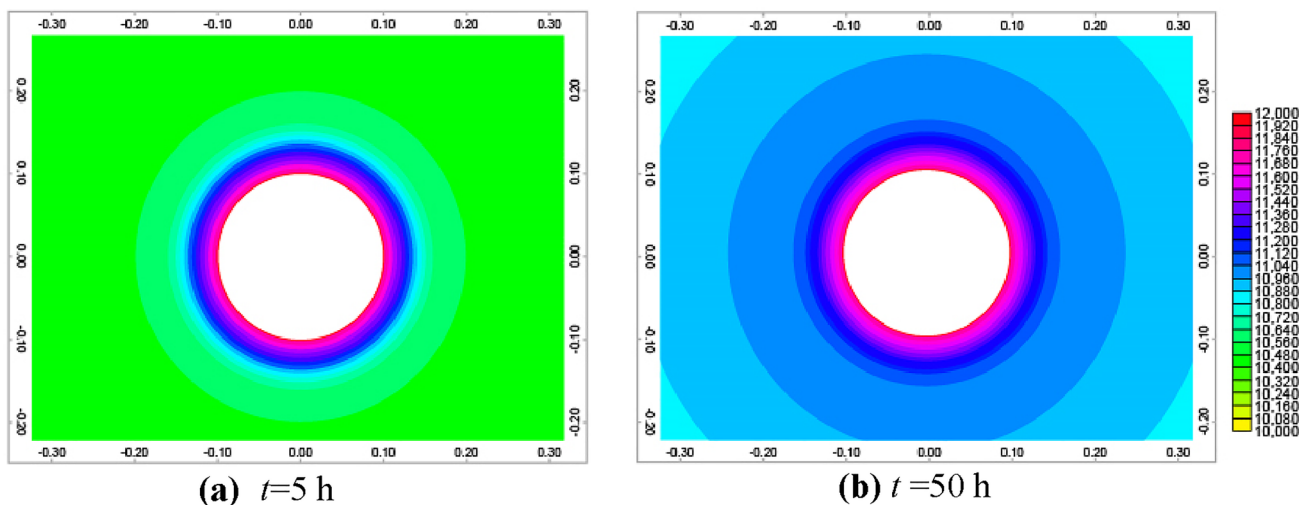


Fig. 15 Formation pressure distribution at the permeability of external filter cake of 0.1 mD

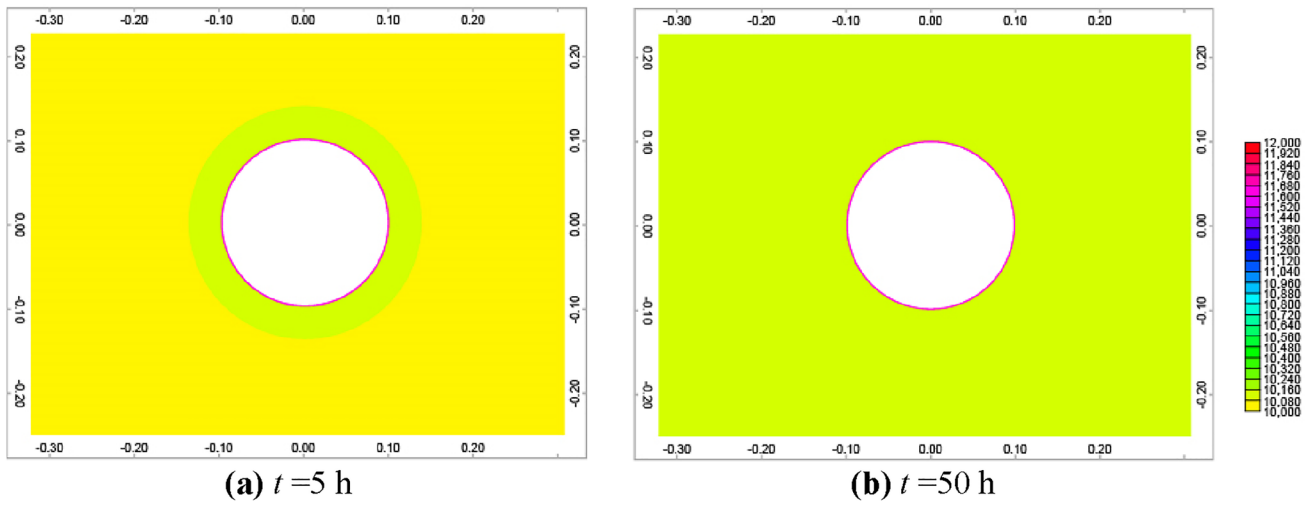


Fig. 16 Formation pressure distribution at the permeability of external filter cake of 0.01 mD

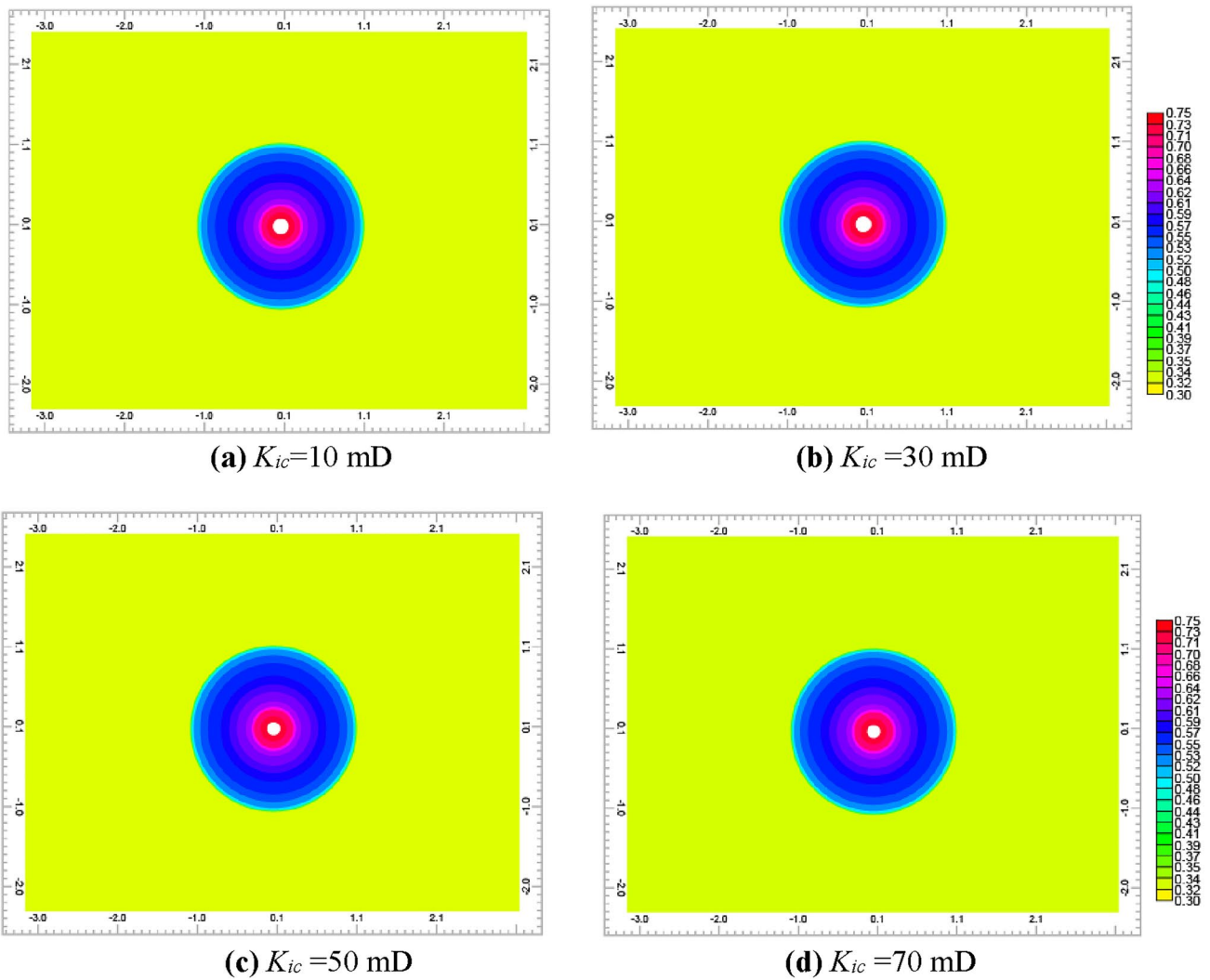
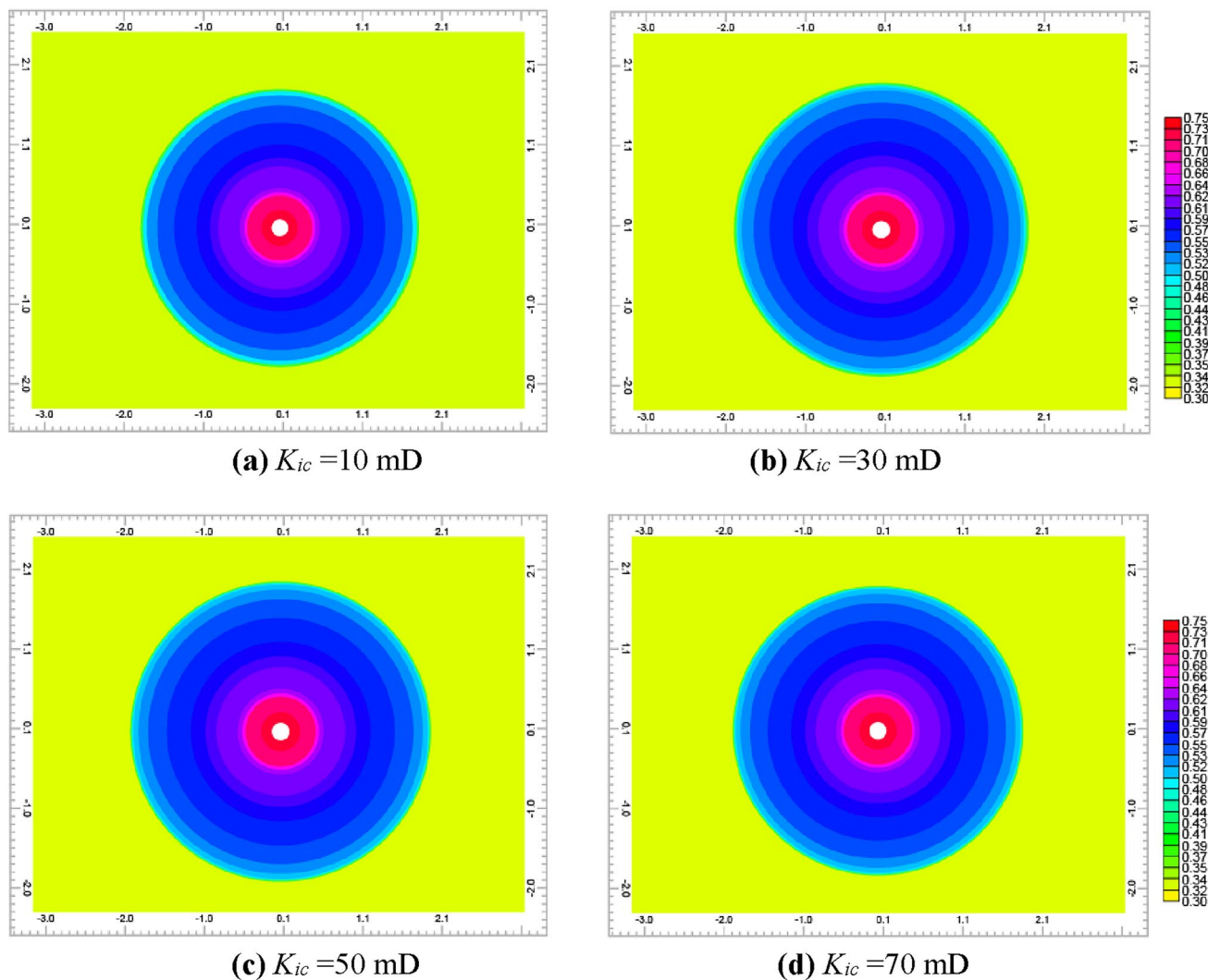


Fig. 17 Filtration under different permeability of internal filter cake at the permeability of external filter cake of 0.01 mD



**Fig. 18** Filtration under different permeability of internal filter cake at the permeability of external filter cake of 0.1 mD

**Table 5** Filtration under different permeability of external and internal filter cake

$K_{ec}/\text{mD}$	$K_{ic}/\text{mD}$	Filtration loss/ $\text{m}^3$
0.01	10	0.278248
	30	0.284062
	50	0.285116
	70	0.285608
0.1	10	1.65999
	30	1.88619
	50	1.94139
	70	1.96707

filter cake permeability has a larger effect on the filtration loss when the external filter cake permeability is 0.10 mD, because when the external filter cake permeability is low, the

pressure consumed by the external filter cake accounts for more than 90% of the total pressure difference, which is the main factor to be considered for control of the filtration loss. When the permeability of the external filter cake is larger, the ratio of the consumed pressure to the total pressure difference is smaller than 55%, and the ratio of the pressure consumed by the internal filter cake to the total pressure difference increases. At this time, with the change in the permeability of the internal filter cake, the change in the filter loss becomes more apparent.

**Limitations of the study and recommendations**

The paper studied impact factors during dynamic radial filtration using numerical methods. The factors include internal/external cake permeability, filtration time, filtrate viscosity, and pressure difference. The innovative aspects



of this paper lie in the application of this numerical analysis method. However, dynamic radial filtration is a complex multi-field coupling problem, we cannot restore the whole filtration process with all aspects. This paper focuses on the impact factors evolution using numerical simulation. Based on the analysis in this paper, we can see that internal filter cake permeability, pressure difference, and filtrate viscosity have a great impact on the filtrate loss during drilling. The proposed simulation method will undoubtedly be effective to improve the understanding of filtrate loss for drilling fluid, and be beneficial for drilling fluid and drilling parameters design; however, there are also some parts of the method need to be improved, and these are also future research interest for us, specific as follows:

- (1) In this paper, the formation temperature, permeability, porosity, stress is assumed to be constant values, the heat exchange-related issues, and formation damage are simplified, such as the change of the drilling fluid's properties and the change of the formation properties after formation damage caused by drilling fluid.
- (2) The model in this paper does not consider the changes of drilling fluid and filtrate fluid in the process of drilling. The change of composition and concentration of the drilling fluid surely have impacts on the drilling filtrate, pressure difference, and the formation properties, which needs further research in future.
- (3) This study only performed one-way filter loss experiments, a radial drilling fluid loss, especially with multi-field effects, is necessary for the drilling filtration and formation damage research.

## Conclusions

- (1) This paper established an innovative numerical analysis method for radial filtration loss using CMG, which can be conveniently applied to the drilling fluid loss study, not only limited to the impact factors analysis in this paper, but also can be used as filtration effect analysis, formation damage analysis, etc.
- (2) External filter cake permeability is an important factor in controlling filtration loss. The pressure consumed by the external filter cake with a lower permeability can account for more than 90% of the total pressure difference. When the external filter cake permeability is high, the internal filter cake permeability significantly affects the dynamic filtration loss of the drilling fluid.
- (3) The dynamic filtration loss of the radial filtration loss for drilling fluid under the formation conditions is still proportional to the filtration time and pressure difference and inversely proportional to the drilling fluid filtrate viscosity. The filtration loss increases with the

external filter cake permeability, but the increment gradually decreases.

- (4) Pressure transferred to the boundary very quickly in numerical simulation. The pressure at the same position in the formation increases gradually with time; however, the increase is relatively small, and the filtration loss rate is essentially constant.

**Acknowledgements** This work is supported by the key laboratory of the Ministry of Education for improving oil and gas recovery of north-east petroleum university and the author would like to appreciate the help from supervisor.

**Funding** This manuscript is supported by the Heilongjiang Provincial Natural Science Foundation of China, LH2022E026.

## Declarations

**Conflict of interest** The authors declare no competing financial interest.

**Open Access** This article is licensed under a Creative Commons Attribution 4.0 International License, which permits use, sharing, adaptation, distribution and reproduction in any medium or format, as long as you give appropriate credit to the original author(s) and the source, provide a link to the Creative Commons licence, and indicate if changes were made. The images or other third party material in this article are included in the article's Creative Commons licence, unless indicated otherwise in a credit line to the material. If material is not included in the article's Creative Commons licence and your intended use is not permitted by statutory regulation or exceeds the permitted use, you will need to obtain permission directly from the copyright holder. To view a copy of this licence, visit <http://creativecommons.org/licenses/by/4.0/>.

## References

- Ahmad HM, Kamal MS, Al-Harathi MA (2018) Rheological and filtration properties of clay-polymer systems: impact of polymer structure. *Appl Clay Sci* 160:226–237. <https://doi.org/10.1016/j.clay.2018.01.016>
- Albattar R, Hoteit H (2019) Modeling yield-power-law drilling fluid loss in fractured formation. *J Petrol Sci Eng* 182:106273. <https://doi.org/10.1016/j.petrol.2019.106273>
- Albattar R, Hoteit H (2021) A semi-analytical approach to model drilling fluid leakage into fractured formation. *Rheol Acta* 60(6–7):353–370. <https://doi.org/10.1007/s00397-021-01275-3>
- Al-Hameedi AT, Alkinani HH, Dunn-Norman S, Albazzaz HW, Alkhamis MM (2019) Insights into eco-friendly and conventional drilling additives: applications, cost analysis, health, safety, and environmental considerations. *Soc Petrol Eng*. <https://doi.org/10.2118/195398-MS>
- Amadi-Echendu J, Yakubu AE (2012) Asset operations: non-productive times during oil well drilling. In: *Proceedings of the 7th world congress on engineering asset management (WCEAM 2012)*. Springer, pp 43–48. [https://doi.org/10.1007/978-3-319-06966-1\\_4](https://doi.org/10.1007/978-3-319-06966-1_4)
- Bahrami H, Rezaee MR, Nazhat DH, Ostojic J, Jamili A (2011) Effect of water blocking damage on flow efficiency and productivity in tight gas reservoirs. In: *SPE production and operations symposium*, Oklahoma City, Oklahoma. SPE-142283-MS. <https://doi.org/10.2118/142283-MS>

- Byrne MT, Jimenez MA, RojasJuan EA, Chavez C (2010) Modeling well inflow potential in three dimensions using computational fluid dynamics. In: SPE international symposium and exhibition on formation damage control, Lafayette, Louisiana. SPE-128082-MS. <https://doi.org/10.2118/128082-MS>
- Ding TW, Yan JN, Feng J (2007) Experimental study on water-based drilling fluids resisting high temperature with high density. *J China Univ Petrol* (edition of Natural Science) 31(2):73–78. <https://doi.org/10.1007/bf03187441>
- Dokhani V, Ma Y, Geng T, Li Z, Yu M (2020) Transient analysis of mud loss in fractured formations. *J Petrol Sci Eng* 195:107722. <https://doi.org/10.1016/j.petrol.2020.107722>
- Fan YR, Wang XL, Wu ZG, Wu JC, Jia JT (2018) Simulation study on drilling fluid invasion considering formation damage. *J Well Logging Technology* 42(04):383–389
- Kemerli M, Engin T (2021) Numerical analysis of a monotube mixed mode magnetorheological damper by using a new rheological approach in CFD. *Rheologica Acta*. <https://doi.org/10.1007/s00397-020-01252-2>
- Kuang SH, Pu XL, Liu YL (2010) Principles of controlling wall building properties of ultra-high-density water based drilling fluid. *J Drill Fluid Completion Fluid* 27(5):8–11
- Lu SQ, Xu TT, Li SR (2006) Study on the factors affecting the dynamic filtration loss of porous sandstone by drilling fluid. *J Drill Fluid Completion Fluid* 03:14–19
- Majidi R, Miska SZ, Ahmed R, Yu M, Thompson LG (2010) Radial flow of yield power-law fluids: numerical analysis, experimental study and the application for drilling fluid losses in fractured formations. *J Pet Sci Eng* 70(3–4):334–343. <https://doi.org/10.1016/j.petrol.2009.12.005>
- Martins AL, Waldmann ATA, Cunha Ribeiro DD, Massarani G (2007) Numerical simulation of the radial viscoelastic flow of a solids free drill in fluid. In: European formation damage conference, Scheveningen, Netherlands. SPE-107617-MS. <https://doi.org/10.2118/107617-MS>
- Okoro EE, Okafor IS, Sanni SE, Obomanu T, Oguntade T, Orodu OD (2020) Investigation of reservoir permeability impairment when drilling with nano treated drill-in mud system. In: SPE Nigeria annual international conference and exhibition, NAIC 2020. SPE-203749-MS. <https://doi.org/10.2118/203749-MS>
- Seyedmohammadi J (2017) The effects of drilling fluids and environment protection from pollutants using some models. *Model Earth Syst Environ* 3(1):23. <https://doi.org/10.1007/s40808-017-0299-7>
- Shan WJ, Tao SX, Fu F, Yue WM, Zhao ZT (2014) Research on the drilling fluid technology for high temperature over 240 °C. *Procedia Eng* 73:218–229. <https://doi.org/10.1016/j.proeng.2014.06.191>
- Soares ASF, Sousa AMFD, Calada LA, Scheid CM, Marques MRC (2021) Study of materials to combat loss of circulation in fractures and static filtration. *J Petrol Sci Eng* 200:108401. <https://doi.org/10.1016/J.PETROL.2021.108401>
- Wang K, Lou Z, Guan L, Zhang X, Qin B, Huang Y (2020a) Experimental study on the performance of drilling fluid for coal seam methane drainage boreholes. *Process Saf Environ Prot* 138(June):246–255. <https://doi.org/10.1016/j.psep.2020.03.041>
- Wang M, Guo Y, Chen W (2020b) Effect of solid particles on the lost circulation of drilling fluid: a numerical simulation. *Powder Technol* 363:408–418. <https://doi.org/10.1016/j.powtec.2019.12.029>
- Won S, Bilgesu HI, Ameri S (2008) Investigation of mud-filtrate invasion using computational fluid dynamics. In: SPE eastern regional/AAPG eastern section joint meeting, Pittsburgh, Pennsylvania. SPE-117769-MS. <https://doi.org/10.2118/117769-MS>
- Yan JN (2011) *Drilling fluid technology* (Revised edition). China University of Petroleum Press, Beijing, pp 88–103

**Publisher's Note** Springer Nature remains neutral with regard to jurisdictional claims in published maps and institutional affiliations.